Chemical Science

ROYAL SOCIETY OF CHEMISTRY

EDGE ARTICLE

View Article Online
View Journal | View Issue

Open Access Article. Published on 04 November 2025. Downloaded on 5/21/2026 3:01:53 PM.
This article is licensed under a Creative Commons Attribution-NonCommercial 3.0 Unported Licence.

Check for updates

Cite this: *Chem. Sci.*, 2026, **17**, 240

All publication charges for this article have been paid for by the Royal Society of Chemistry

Received 21st October 2025
Accepted 3rd November 2025

DOI: 10.1039/d5sc08143b

rsc.li/chemical-science

Catalytic asymmetric construction of remote P or other heteroatom (Si/S) stereogenic axially chiral scaffolds

Wenqi Liu, Zhijie Ling, Yang-Zi Liu * and Wei-Ping Deng *

Axial chirality represents a fundamental element of stereochemistry and is a defining structural feature in many chiral compounds. Although the axial chirality of atropisomers, allenes and spiranes has been extensively studied, the chemistry of alkylidenecycloalkanes and their analogues—especially those possessing P-, S- or Si-based axial chirality—remains underdeveloped. Here we report a chiral phosphoric acid-catalyzed oxime condensation that enables the construction of remote heteroatom (P/S/Si)-stereogenic axially chiral scaffolds. The reaction accommodates a broad range of functional groups, delivering optically active axially chiral 9-heteroanthrone-based oxime ethers in good to excellent enantioselectivities (up to 98 : 2 er). We also describe a modular synthesis of dibenzoazaphosphepinones and demonstrate their application as chiral monodentate phosphine ligands in asymmetric catalysis.

Introduction

Axially chiral compounds have garnered significant attention in synthetic[1,2] and pharmaceutical[3] chemistry due to their presence in natural products and diverse applications[4–6] as bioactive drug molecules,[7–9] chiral ligands and catalysts,[10,11] and functional materials like liquid crystals.[12] Advances in catalytic asymmetric synthesis over recent decades have established robust methods for constructing axially chiral compounds, particularly (hetero)aryl-based X–Y (X, Y = C, N) systems[13–31] and allenes,[32–34] making this a vibrant subfield within asymmetric catalysis. These advances have stimulated exploration of novel axially chiral skeletons.[22,30,35–37] In contrast to classical atropisomers, allenes and spiranes constitute a distinct class of non-atropisomeric axially chiral compounds that has recently garnered increasing attention.[34] The hybridization of alkene and spirane structural motifs gives rise to a distinctive class of non-atropisomeric axial stereoisomerism, termed alkylidenecyclic molecules. However, investigation into this axial stereoisomerism is still limited[36,37] (Scheme 1A). Early synthetic approaches to such architectures typically relied on non-catalytic methods.[38–44] A landmark study by Fiaud *et al.* in 1988 described the enantioselective synthesis of 4-alkylcyclohexylbenzene derivatives *via* asymmetric palladium catalysis,[45] yet this strategy remained largely overlooked for years. Recently, more efficient routes to these novel skeletons have emerged, including: (i) photochemical deracemization of racemic alkylidenecycloalkanes;[46,47] (ii) enantioselective [2 + 2] cycloadditions between terminal alkenes and allenoates or allenyl imides;[48,49] (iii) transition metal-catalyzed desymmetrization of functionalized cycloalkanes;[50–61] and (iv) enantioselective functionalization of cyclic carbonyl compounds[62–71] (Scheme 1B).

Notably, the construction of axially chiral tricyclic aromatic scaffolds bearing remote heteroatom (P/S/Si)-stereogenic centers remains rare. This may be attributed to the challenge of exercising stereocontrol at distal heteroatom sites: while desymmetrization of monocyclic substrates enables effective control of carbon stereocenters, the bulky tricyclic aromatic framework complicates stereochemical manipulation at remote P/S/Si centres.[66] Moreover, substitution of distal carbon atoms with phosphorus, sulfur or silicon elongates the $C(sp^2)$–$P(sp^3)$, $C(sp^2)$–$S(sp^3)$, $C(sp^2)$–$Si(sp^3)$ bonds relative to $C(sp^2)$–$C(sp^3)$, increasing ring strain and conformational constraint. The inherent structural distortion in 9-heteroanthrones may further complicate precise stereochemical control[72] (Scheme 1C).

Inspired by these precedents and the potential applications of 9-heteroanthrones,[73–76] we envisioned a chiral phosphoric acid-catalyzed enantioselective condensation between 9-heteroanthrones and hydroxylamines to construct axially chiral 9-heteroanthrone-based oxime ethers (Scheme 1D). We proposed that stereocontrol in this condensation would arise during the dehydration step, wherein the CPA catalyst engages the NH group *via* hydrogen bonding and activates the hydroxyl group through protonation to facilitate water elimination[65] (Scheme 1C). Moreover, in this work, we also developed a modular synthesis of dibenzoazaphosphepinones *via* axial-to-point chirality conversion from 9-phosphaanthrone-derived

Key Laboratory of the Ministry of Education for Advanced Catalysis Materials, College of Chemistry and Materials Science, Zhejiang Normal University, 688 Yingbin Road, Jinhua, Zhejiang 321004, China. E-mail: liuyangzi@zjun.edu.cn; dengwp827@zjnu.edu.cn

© 2026 The Author(s). Published by the Royal Society of Chemistry

Open Access Article. Published on 04 November 2025. Downloaded on 5/21/2026 3:01:53 PM.
This article is licensed under a Creative Commons Attribution-NonCommercial 3.0 Unported Licence.

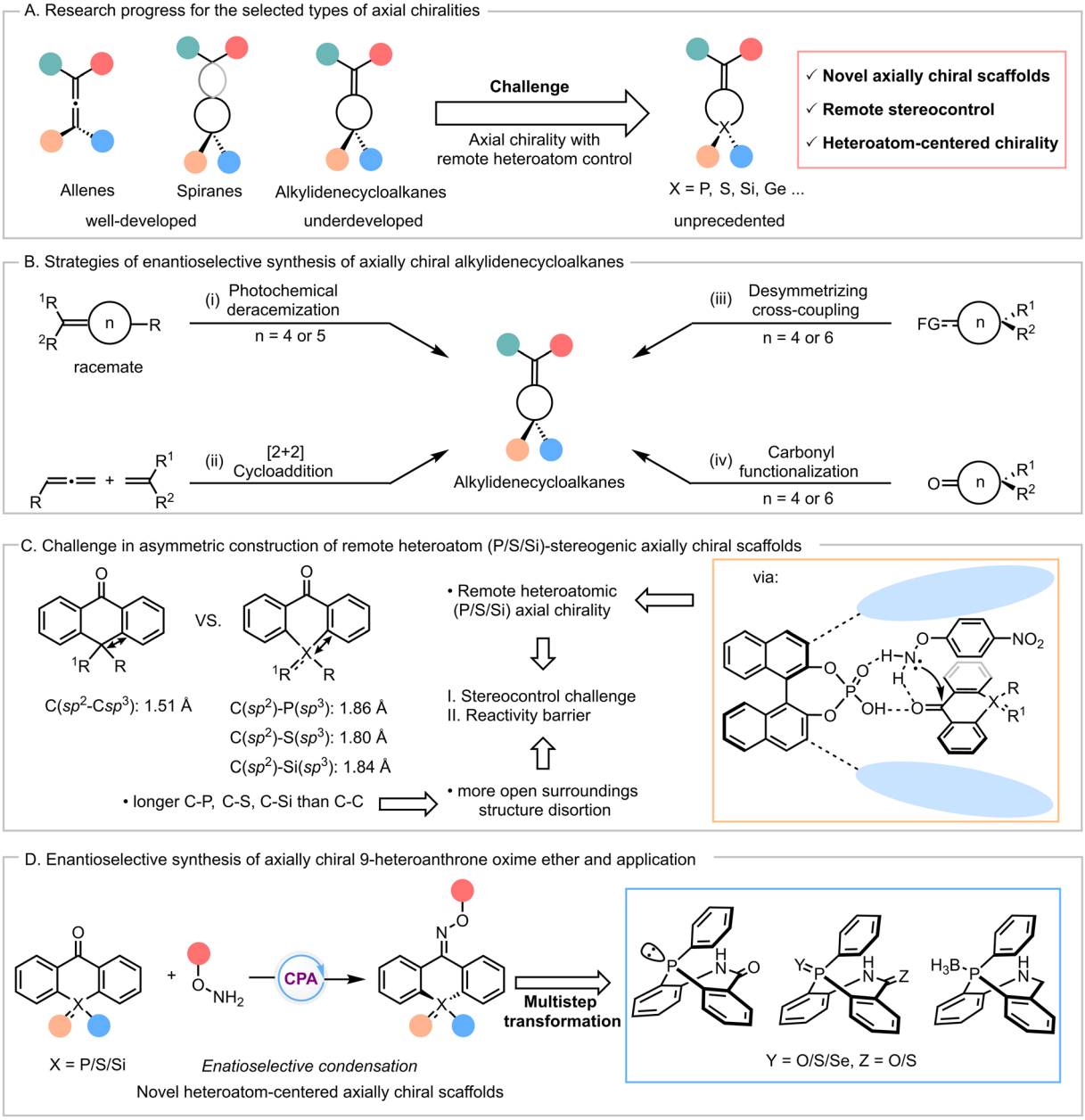

Scheme 1 Enantioselective synthesis of axially chiral alkylidenecycloalkanes.

oxime ethers and explored their applications as chiral monodentate phosphine ligands in asymmetric reactions (Scheme 1D).

Results and discussion

We began our investigation by examining the model reaction between 5-phenyl-10*H*-acridophosphin-10-one 5-oxide (**1a**) and *O*-(4-nitrophenyl)hydroxylamine (**2a**) using a series of chiral phosphoric acid (CPA) catalysts with varied scaffold structures in DCE at 60 °C (Table 1, entries 1–7). The less sterically encumbered CPA **C1** afforded only trace product (entry 1). Pleasingly, **C2** delivered the target product **3a** in 65% yield with 93.5 : 6.5 enantiomeric ratio (er) (entry 2). Both the 2,4,6-tricyclohexyl-substituted **C3** and the 9-phenanthrenyl-based **C4** afforded moderate enantioselectivity (85 : 15–87.5 : 12.5 er) but with diminished yields (entries 3–4). The 8*H*-binaphthyl-derived CPA **C5** provided acceptable yield and er (entry 5). The 2,4,6-triisopropyl-substituted spirocyclic CPA **C6** yielded only trace product (entry 6), whereas the 9-phenanthrenyl-substituted spirocyclic CPA **C7** afforded good enantioselectivity (93 : 7 er) with 79% yield (entry 7). Subsequent solvent screening identified CCl_4 as the optimal choice, delivering improved enantioselectivity (97 : 3 er, entries 8–15). Reducing the temperature to 50 °C maintained high stereocontrol but lowered the yield (75%, entry 16). Omitting molecular sieves or reducing the catalyst loading adversely affected reaction efficiency (55–67%, entries 17 and 18). Further optimization (see SI) established the

Open Access Article. Published on 04 November 2025. Downloaded on 5/21/2026 3:01:53 PM. This article is licensed under a Creative Commons Attribution-NonCommercial 3.0 Unported Licence.

Table 1 Optimization of the reaction conditions[a]

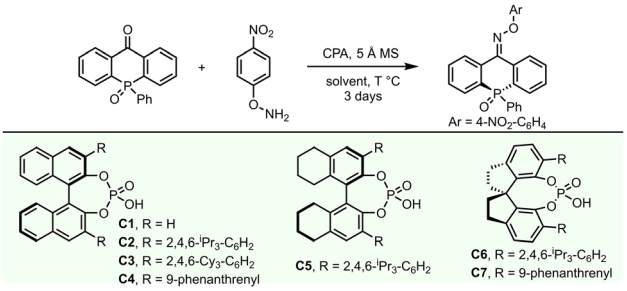

Entry	CPA	Solvent	Yield[b] (%)	er[c] (%)
1	**C1**	DCE	Trace	—
2	**C2**	DCE	65	93.5 : 6.5
3	**C3**	DCE	49	87.5 : 12.5
4	**C4**	DCE	12	85 : 15
5	**C5**	DCE	57	92.5 : 7.5
6	**C6**	DCE	Trace	—
7	**C7**	DCE	79	93 : 7
8	**C2**	PhCl	63	89 : 11
9	**C2**	$PhCF_3$	83	87.5 : 12.5
10	**C2**	Toluene	65	91 : 9
11	**C2**	DCM	57	93.5 : 6.5
12	**C2**	$CHCl_3$	47	82 : 18
13	**C2**	CCl_4	99	97 : 3
14	**C2**	THF	Trace	—
15	**C2**	Decaline	35	95 : 5
16[d]	**C2**	CCl_4	75	96.5 : 3.5
17[e]	**C2**	CCl_4	55	96 : 4
18[f]	**C2**	CCl_4	67	96.5 : 3.5

[a] Reaction conditions: **1a** (0.10 mmol), **2a** (0.12 mmol), CPA (10 mol%) and 5 Å molecular sieves (50 mg) in solvent (0.3 mL) at 60 °C for 72 h unless otherwise noted. [b] Isolated yield. [c] Enantiomeric ratio (er) determined by chiral HPLC analysis. [d] Reaction performed at 50 °C. [e] Without 5 Å molecular sieves. [f] With 5 mol% catalyst loading.

standard conditions: **C2** (10 mol%) and 5 Å molecular sieves (50 mg) in CCl_4 (0.3 mL) at 60 °C for 72 hours.

With optimized conditions in hand, we first explored the substrate scope with respect to the hydroxylamine component (Table 2, A). Using *O*-(4-*tert*-butylphenyl)hydroxylamine (**2b**) afforded oxime ether **3b** in 93% yield and 97 : 3 er. A phenyl substituent at the *para*-position gave **3c** in 85% yield with 95 : 5 er. Hydroxylamines bearing an OCF_3 group provided **3d** in 92% yield and 95.5 : 4.5 er. Other electron-withdrawing *para*-substituents—halogen (**2e**), ester (**2f**) and cyano (**2g**)—participated effectively, yielding products (**3e–3g**) with high stereoselectivity (90–93% yield, 94.5 : 5.5–96.5 : 3.5 er). *meta*-Bromo (**2i**) and ester (**2j**) substituents also afforded excellent stereocontrol (94.5 : 5.5 and 96.5 : 3.5 er, respectively), while a *meta*-methoxy group (**2h**) led to lower er (89.5 : 10.5) and yield (75%), likely due to its electron-donating character. *ortho*-Substitution (**2k**) compromised both enantioselectivity (87 : 13 er) and yield (76%), presumably due to steric hindrance. Benzyl-substituted hydroxylamine **2p** (95% yield, 90.5 : 9.5 er) and aliphatic allylic hydroxylamine **2q** (85% yield, 88.5 : 11.5 er) also underwent efficient condensation with the selected 9-phosphaanthrone (**1a**). Absolute configurations were assigned based on X-ray crystallographic analysis of **3a** (CCDC 2478635).

Given its superior reactivity and ease of product isolation, *O*-(4-*tert*-butylphenyl)hydroxylamine (**2b**) was selected to evaluate the substrate scope of 9-heteroanthrones (Table 2, B). *para*-Substituted electron-donating methyl or methoxy groups on phenyl group afforded **3r** and **3s** in excellent yields (90–92%) and enantioselectivities (94 : 6–96 : 4 er). The condensation tolerated electron-withdrawing *para*-substituents, including halogens and trifluoromethyl groups, yielding products **3t–3v** with high enantioselectivity (95 : 5–96 : 4 er). Oxime ethers **3w** and **3x** were obtained in good yields (84–91%) from *meta*-substituted methyl and chlorophenyl groups. *ortho*-Methyl group afforded **3y** in 89% yield and 94.5 : 5.5 er. 3,5-Dimethylphenyl 9-phosphaanthrone reacted smoothly to give **3z** (86% yield, 96 : 4 er). Reaction of cyclohexyl 9-phosphaanthracene or phosphoramidate proceeded in 80–85% yield to give **3aa** or **3ab** with excellent stereoselectivity (97 : 3–98 : 2 er). By contrast, 3,6- or 2,7-dimethyl-substituted 9-phosphaanthrone provided **3ac** or **3ad** in moderate yields (55–62%) but good enantioselectivities (91 : 9–94.5 : 5.5 er). To further demonstrate generality, we investigated the desymmetrization of 9-Si-anthrones (**1ba**, **1bb**) and a 9-S-anthrone (**1ca**) for constructing remote S/Si-stereogenic axially chiral scaffolds (see SI for condition screening). Axially chiral 9-Si-anthrone-based oxime ethers (**3ba**, **3bb**) were obtained in excellent yields with moderate to good er (83.5 : 16.5–86.5 : 13.5). The 9-S-anthrone (**1ca**) reacted smoothly, delivering the product (**3ca**) in moderate yield (69%) with moderate enantioselectivity (79 : 21 er) (Table 2, B). The consistently lower enantioselectivities observed for these S- and Si-containing scaffolds compared to their phosphorus analogues prompt us to consider factors beyond bond length considerations, such as the steric hindrance of substituents and other secondary effects.

We next investigated the conversion of remote phosphorus axial chirality to phosphorus-centered chirality *via* a Beckmann rearrangement. Pd-catalyzed deallylation of **3q** (88 : 12 er) afforded hydroxylamine **4**, which underwent a Beckmann rearrangement to give intermediate **5** (82% over two steps, 83 : 17 er). The slight erosion in enantioselectivity may be attributed to facile isomerization of the hydroxyl group in **4**. Standing at room temperature for 24 h converted compound **5** to **7b**, and subsequent trichlorosilane reduction afforded **6a** in 60% yield over two steps (82.5 : 17.5 er). Recrystallization yielded enantiopure *R*-**6a** (>99.5 : 0.5 er), the structure of which was confirmed by X-ray crystallography (CCDC 2478637). Reduction of *R*-**6a** with a borane-dimethyl sulfide complex gave **7a** in 65% yield with retained er (>99.5 : 0.5). The P(III) center in *R*-**6a** was oxidatively functionalized using H_2O_2, S_8 and Se to furnish **7b**, **7c** and **7d**, respectively, in excellent yields (94–99%) with complete chirality retention (>99.5 : 0.5 er). Treatment of **7b** with Lawesson's reagent afforded thioamide **8a** in 90% yield and 99 : 1 er. Methylation of **8a** gave **9a** quantitatively (99%) with 99.5 : 0.5 er. These transformations highlight the versatility of the method for accessing diverse functionalized products with high efficiency and stereochemical fidelity (Scheme 2).

© 2026 The Author(s). Published by the Royal Society of Chemistry

Open Access Article. Published on 04 November 2025. Downloaded on 5/21/2026 3:01:53 PM. This article is licensed under a Creative Commons Attribution-NonCommercial 3.0 Unported Licence.

Table 2 Substrate scope with respect to 9-heteroanthrone derivatives and hydroxylamines

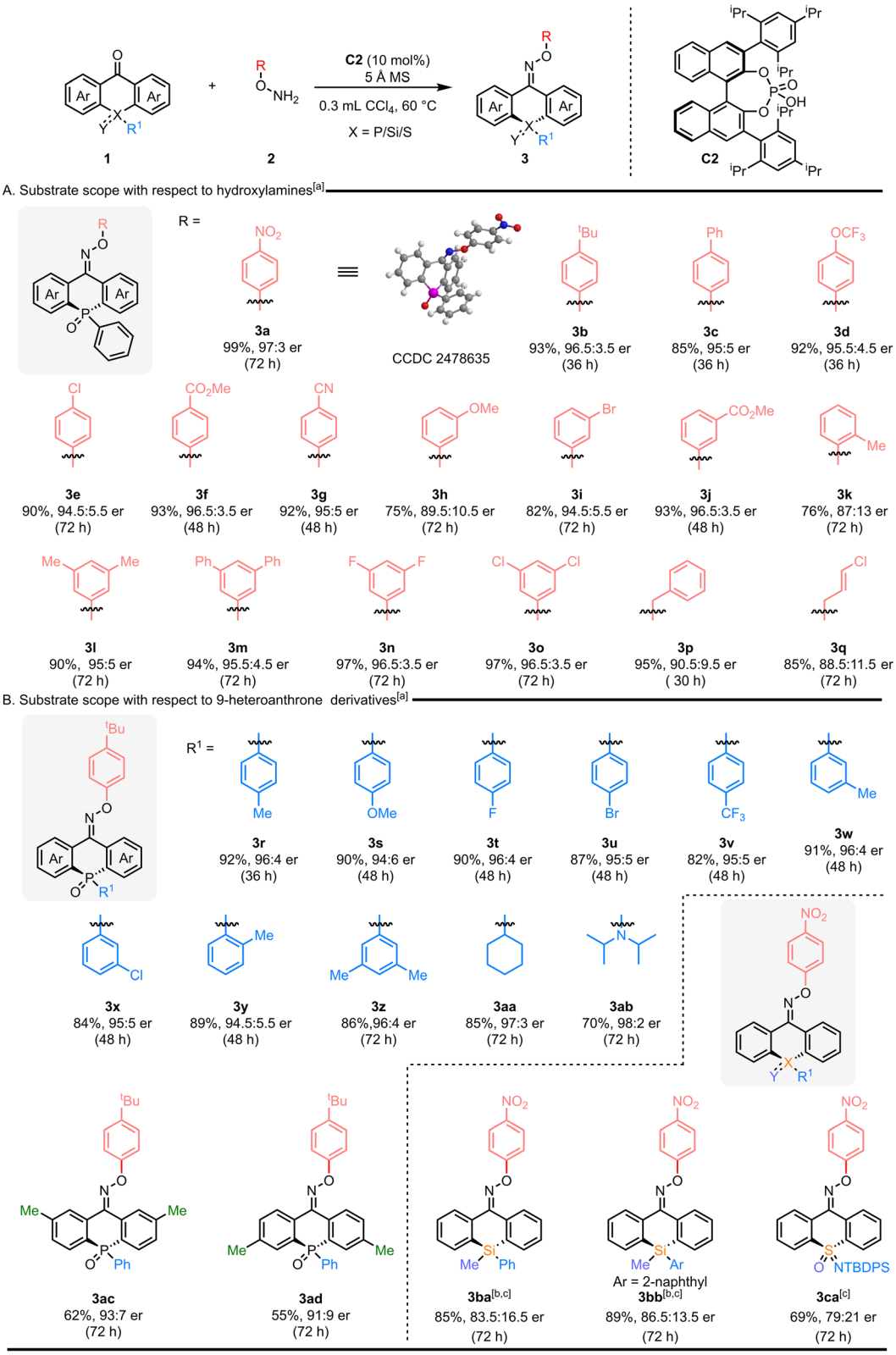

[a] Reaction conditions: (**1**) (0.10 mmol), (**2**) (0.12 mmol), (**C2**) (10 mol%) and 5 Å molecular sieves (50 mg) in solvent (0.3 mL) at 60 °C. Yields are isolated. The er determined by chiral HPLC analysis. [b] Na_2SO_4 used instead of 5 Å molecular sieves. [c] Decaline instead of CCl_4.

Open Access Article. Published on 04 November 2025. Downloaded on 5/21/2026 3:01:53 PM.
This article is licensed under a Creative Commons Attribution-NonCommercial 3.0 Unported Licence.

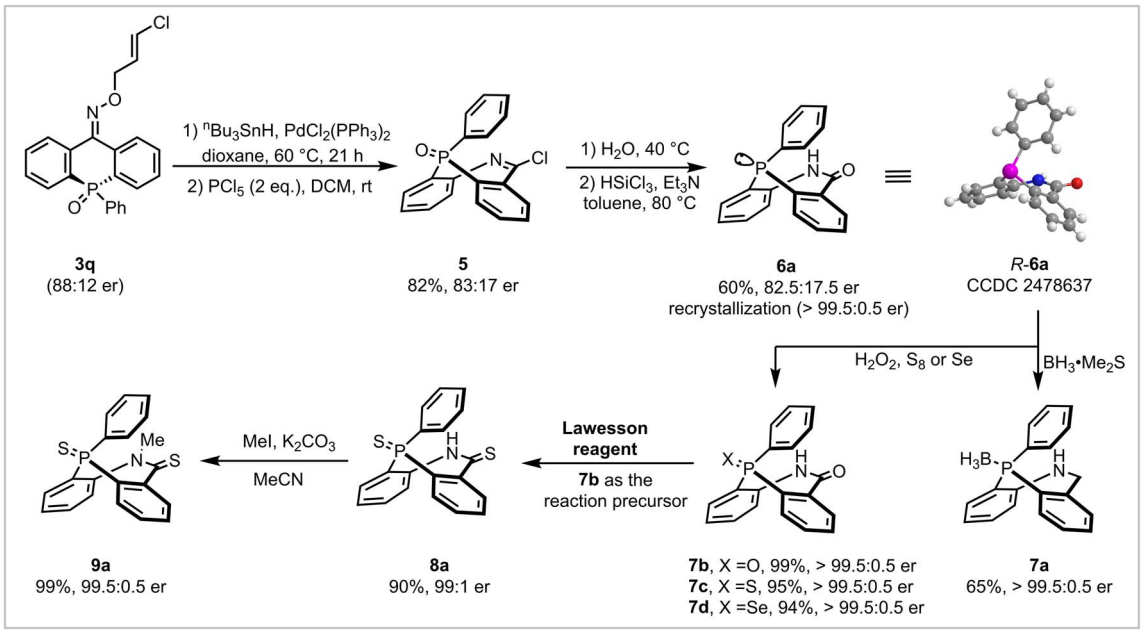

Scheme 2 Synthetic transformations of **3q**.

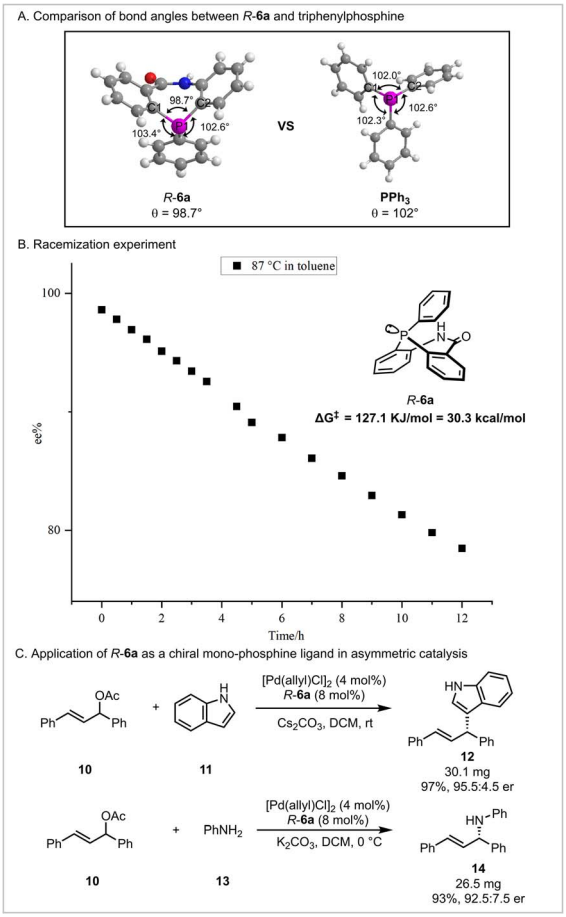

Scheme 3 The bond angle analysis, racemization studies, and synthetic application of cyclic triarylphosphine **6a**.

Furthermore, we present *R*-**6a**—a novel cyclic triarylphosphine scaffold that was previously inaccessible in enantiopure form through conventional synthetic routes. In contrast to conventional triarylphosphines, this structure exhibits a narrower ∠C1P1C2 bond angle (98.7° *vs.* 102.0°) and enhanced rigidity, features that are anticipated to enhance its performance in asymmetric catalysis (Scheme 3A). Racemization studies revealed a high inversion barrier of 30.3 kcal mol^{-1} for *R*-**6a** in toluene at 87 °C (Scheme 3B). Notably, *R*-**6a** (>99.5 : 0.5 er) functioned effectively as a chiral monodentate phosphine ligand in Pd-catalyzed asymmetric allylic alkylation (Scheme 3C). For instance, the reaction of indole with (*E*)-1,2-diphenylallyl acetate **10** delivered the C3-phenylallyl-substituted indole **12** in 97% yield and 95.5 : 4.5 er. Similarly, using benzylamine **13** as the nucleophile afforded product **14** in 93% yield and 92.5 : 7.5 er. The absolute configurations of **12** and **14** were assigned based on literature reports.[77,78] These results underscore the promising potential of cyclic chiral triarylphosphines in the field of asymmetric catalysis.

Conclusions

In summary, we have established an efficient and enantioselective construction of remote P/S/Si-stereogenic axially chiral frameworks from 9-heteroanthrones and hydroxylamines *via* chiral phosphoric acid-catalyzed asymmetric condensation. This work overcomes longstanding challenges in stereocontrol at distal heteroatom centers and provides access to a novel class of axially chiral oxime ethers in high enantiopurity (up to 98 : 2 er). Furthermore, these products serve as versatile platforms for diversity-oriented synthesis: through a Beckmann rearrangement, axial chirality is efficiently converted into phosphorus-centered point chirality, yielding enantioenriched

© 2026 The Author(s). Published by the Royal Society of Chemistry

Open Access Article. Published on 04 November 2025. Downloaded on 5/21/2026 3:01:53 PM. This article is licensed under a Creative Commons Attribution-NonCommercial 3.0 Unported Licence.

dibenzoazaphosphepinones. The resulting cyclic triarylphosphine architecture not only exhibits enhanced rigidity and configurational stability but also functions as an effective chiral monodentate ligand, demonstrating promising utility in catalytic asymmetric allylation reaction. This work opens avenues for the design and application of heteroatom axially chiral systems in synthesis and catalysis.

Author contributions

W. L. performed most of the experiments, with support from Z. L. in the catalyst and substrate preparation. W. L., Y.-Z. L. and W.-P. D. conceived of the idea and designed the experiments. W. L., Y.-Z. L. and W.-P. D. wrote the manuscript. Y.-Z. L. and W.-P. D. directed the project. All authors contributed to discussions.

Conflicts of interest

There are no conficts to declare.

Data availability

CCDC 2478635 (**3a**) and 2478637 (**6a**) contain the supplementary crystallographic data for this paper.[79a,b]

The data supporting this article have been included as part of the supplementary information (SI). Supplementary information: experimental procedures, characterization data, NMR spectra, HPLC traces, and additional figures supporting the results presented in the main text. See DOI: **https://doi.org/10.1039/d5sc08143b**.

Acknowledgements

We are grateful for the financial support from the Leading Innovative and Entrepreneur Team Introduction Program of Zhejiang (2022R01007), the NSFC (22201253), and the Start-up Research Grant from Zhejiang Normal University.

Notes and references

1 J. M. Lassaletta, *Atropisomerism and Axial Chirality*, World Scientific, Singapore, 2019.
2 Y.-B. Wang and B. Tan, *Acc. Chem. Res.*, 2018, **51**, 534–547.
3 M. Basilaia, M. H. Chen, J. Secka and J. L. Gustafson, *Acc. Chem. Res.*, 2022, **55**, 2904–2919.
4 J. E. Smyth, N. M. Butler and P. A. Keller, *Nat. Prod. Rep.*, 2015, **32**, 1562–1583.
5 G. Bringmann, T. Gulder, T. A. M. Gulder and M. Breuning, *Chem. Rev.*, 2011, **111**, 563–639.
6 S. R. LaPlante, L. D. Fader, K. R. Fandrick, D. R. Fandrick, O. Hucke, R. Kemper, S. P. F. Miller and P. J. Edwards, *J. Med. Chem.*, 2011, **54**, 7005–7022.
7 S. T. Toenjes and J. L. Gustafson, *Future Med. Chem.*, 2018, **10**, 409–422.
8 J. Clayden, W. J. Moran, P. J. Edwards and S. R. LaPlante, *Angew. Chem., Int. Ed.*, 2009, **48**, 6398–6401.
9 G. Bringmann, A. J. Price Mortimer, P. A. Keller, M. J. Gresser, J. Garner and M. Breuning, *Angew. Chem., Int. Ed.*, 2005, **44**, 5384–5427.
10 Y. Chen, S. Yekta and A. K. Yudin, *Chem. Rev.*, 2003, **103**, 3155–3212.
11 I. O. Betinol, Y. Kuang, B. P. Mulley and J. P. Reid, *Chem. Rev.*, 2025, **125**, 4184–4286.
12 G. Dotsevi, Y. Sogah and D. J. Cram, *J. Am. Chem. Soc.*, 1976, **98**, 3038–3041.
13 G. Liao and B.-F. Shi, *Acc. Chem. Res.*, 2025, **58**, 1562–1579.
14 S. Gao, L. Su and J. Liu, *J. Am. Chem. Soc.*, 2025, **147**, 23946–23956.
15 X. Yang, L. Su, S. Gao and J. Liu, *Angew. Chem., Int. Ed.*, 2025, e202517629.
16 B. Ye, L. Su, K. Zheng, S. Gao and J. Liu, *Angew. Chem., Int. Ed.*, 2025, **64**, e202413949.
17 L. Su, S. Gao and J. Liu, *Nat. Commun.*, 2024, **15**, 7248.
18 T. A. Schmidt, V. Hutskalova and C. Sparr, *Nat. Rev. Chem.*, 2024, **8**, 497–517.
19 H.-H. Zhang, T.-Z. Li, S.-J. Liu and F. Shi, *Angew. Chem., Int. Ed.*, 2024, **63**, e202311053.
20 S.-H. Xiang, W.-Y. Ding, Y. B. Wang and B. Tan, *Nat. Catal.*, 2024, **7**, 483–498.
21 J. Feng, C.-J. Lu and R.-R. Liu, *Acc. Chem. Res.*, 2023, **56**, 2537–2554.
22 W. Qiu, R. Tao, Y. He, Y. Zhou, K. Yang and Q. Song, *Nat. Commun.*, 2024, **15**, 10432.
23 J. K. Cheng, S.-H. Xiang and B. Tan, *Acc. Chem. Res.*, 2022, **55**, 2920–2937.
24 D. Liang, W. Xiao, S. Lakhdar and J. Chen, *Green Synth. Catal.*, 2022, **3**, 212–218.
25 J. K. Cheng, S.-H. Xiang, S. Li, L. Ye and B. Tan, *Chem. Rev.*, 2021, **121**, 4805–4902.
26 J. Wencel-Delord, A. Panossian, F. R. Leroux and F. Colobert, *Chem. Soc. Rev.*, 2015, **44**, 3418–3430.
27 A. Link and C. Sparr, *Chem. Soc. Rev.*, 2018, **47**, 3804–3815.
28 Z.-X. Zhang, T.-Y. Zhai and L.-W. Ye, *Chem Catal.*, 2021, **1**, 1378–1412.
29 Y.-J. Wu, G. Liao and B.-F. Shi, *Green Synth. Catal.*, 2022, **3**, 117–136.
30 G. Centonze, C. Portolani, P. Righi and G. Bencivenni, *Angew. Chem., Int. Ed.*, 2023, **62**, e202303966.
31 D. Wang, J. Zong, B. Wang, L. Sun, X. Xiao, H. Piao, M. Ke and F. Chen, *Green Synth. Catal.*, 2025, **6**, 211–215.
32 W. Su, J. Zhu, Y. Chen, X. Zhang, W. Qiu, K. Yang, P. Yu and Q. Song, *Nat. Chem.*, 2024, **16**, 1312–1319.
33 L. Li, S. Wang, A. Jakhar and Z. Shao, *Green Synth. Catal.*, 2023, **4**, 124–134.
34 R. K. Neff and D. E. Frantz, *ACS Catal.*, 2014, **4**, 519–528.
35 K. Yang, Y. Mao, Z. Zhang, J. Xu, H. Wang, Y. He, P. Yu and Q. Song, *Nat. Commun.*, 2023, **14**, 4438.
36 Z.-L. Wang and Y.-H. Xu, *Synthesis*, 2023, **56**, 1259–1272.
37 F. Hu and Y. Xia, *Eur. J. Org Chem.*, 2023, **26**, e202300151.
38 H. J. Bestmann and J. Lienert, *Angew. Chem., Int. Ed.*, 1969, **8**, 763–764.
39 S. Hanessian, D. Delorme, S. Beaudoin and Y. Leblanc, *J. Am. Chem. Soc.*, 1984, **106**, 5754–5756.

© 2026 The Author(s). Published by the Royal Society of Chemistry

Open Access Article. Published on 04 November 2025. Downloaded on 5/21/2026 3:01:53 PM. This article is licensed under a Creative Commons Attribution-NonCommercial 3.0 Unported Licence.

40 S. E. Denmark and C. T. Chen, *J. Am. Chem. Soc.*, 1992, **114**, 10674–10676.
41 A. Abiko and S. Masamune, *Tetrahedron Lett.*, 1996, **37**, 1077–1080.
42 W.-M. Dai, J. Wu and X. Huang, *Tetrahedron: Asymmetry*, 1997, **8**, 1979–1982.
43 M. Mizuno, K. Fujii and K. Tomioka, *Angew. Chem., Int. Ed.*, 1998, **37**, 515–517.
44 M. Iguchi and K. Tomioka, *Org. Lett.*, 2002, **4**, 4329–4331.
45 J. C. Fiaud and J. Y. Legros, *Tetrahedron Lett.*, 1988, **29**, 2959–2962.
46 T. Kratz, P. Steinbach, S. Breitenlechner, G. Storch, C. Bannwarth and T. Bach, *J. Am. Chem. Soc.*, 2022, **144**, 10133–10138.
47 G. Zeng, W. Shi, Z. Wang, X. Zhao, Y. Yin and Z. Jiang, *J. Am. Chem. Soc.*, 2025, **147**, 26079–26088.
48 J. M. Wahl, M. L. Conner and M. K. Brown, *J. Am. Chem. Soc.*, 2018, **140**, 15943–15949.
49 W. Xiao, L. Ning, S. Xin, S. Dong, X. Liu and X. Feng, *Angew. Chem., Int. Ed.*, 2022, **61**, e202211596.
50 Y. Chen, J. Chen and S. Zhu, *ACS Cent. Sci.*, 2025, **11**, 899–909.
51 S. Wang, J. Liu, W. Ma and Q. Song, *Sci. China Chem.*, 2025, **68**, 1929–1936.
52 B. Wang, J. Zhao, J. Ying, B. Cheng and Z. Lu, *Angew. Chem., Int. Ed.*, 2025, **64**, e202421500.
53 B.-R. Shao, W.-F. Jiang, C. Wang and L. Shi, *Angew. Chem., Int. Ed.*, 2025, **64**, e202421287.
54 B. Gong, Q. Lu, R. Sun, Z. Li, Y. Chen, A. Lin, H. Yao and S. Gao, *ACS Catal.*, 2025, **15**, 2351–2358.
55 J. Hurtado, N. Iragorri, E. Reyes, J. L. Vicario and E. Fernández, *Angew. Chem., Int. Ed.*, 2024, **63**, e202411232.
56 C. Sun, T. Qi, F.-U. Rahman, T. Hayashi and J. Ming, *Nat. Commun.*, 2024, **15**, 9307.
57 S.-J. He, B. Shen, L.-Z. Zuo, S.-H. Xiang, H.-H. Liu, P. Yu and B. Tan, *J. Am. Chem. Soc.*, 2024, **146**, 19137–19145.
58 B.-R. Shao, W.-F. Jiang, C. Zheng and L. Shi, *Chem Catal.*, 2023, **3**, 100697.
59 C. Ma, Y. Sun, S. Liu, Z.-M. Li, J. Yang, H. Guo and J. Zhang, *Chem Catal.*, 2022, **2**, 3196–3206.
60 S. Li, J.-L. Xu and Y.-H. Xu, *Org. Lett.*, 2022, **24**, 6054–6059.
61 J. Janabel, D. Kumar, V. V. Kanale, M. Liu and C. Uyeda, *J. Am. Chem. Soc.*, 2025, **147**, 23270–23276.
62 M. Arnold, J. Hammes, M. Ong, C. Mück-Lichtenfeld and J. M. Wahl, *Angew. Chem., Int. Ed.*, 2025, **64**, e202503056.
63 X.-Y. Wang, X.-Z. Xie, Z.-W. Wu, Y. Bai, Y. Chen and J.-S. Yu, *Synthesis*, 2024, **56**, 3879–3888.
64 J. Z. Essman and E. N. Jacobsen, *J. Am. Chem. Soc.*, 2024, **146**, 7165–7172.
65 M. Ying, K. Wang, W. Yan, M. Pu and L. Lin, *Chem.–Eur J.*, 2024, **30**, e202401243.
66 S.-J. He, S. Zhu, S.-Q. Qiu, W.-Y. Ding, J. K. Cheng, S.-H. Xiang and B. Tan, *Angew. Chem., Int. Ed.*, 2023, **62**, e202213914.
67 S. Zhu, J.-H. Mao, J. K. Cheng, S.-H. Xiang and B. Tan, *Chem*, 2022, **8**, 2529–2541.
68 S. Crotti, N. Di Iorio, C. Artusi, A. Mazzanti, P. Righi and G. Bencivenni, *Org. Lett.*, 2019, **21**, 3013–3017.
69 S. K. Nimmagadda, S. C. Mallojjala, L. Woztas, S. E. Wheeler and J. C. Antilla, *Angew. Chem., Int. Ed.*, 2017, **56**, 2454–2458.
70 L. Gramigna, S. Duce, G. Filippini, M. Fochi, M. C. Franchini and L. Bernardi, *Synlett*, 2011, **18**, 2745–2749.
71 S. Arai, S. Hamaguchi and T. Shioiri, *Tetrahedron Lett.*, 1998, **39**, 2997–3000.
72 Y. Yan, Q. Wei, Z. Su, N.-N. Hang, T. Hayashi and J. Ming, *Nat. Commun.*, 2024, **15**, 9915.
73 M. A. Saucier, N. A. Kruse, B. E. Seidel, N. I. Hammer, G. S. Tschumper and J. H. Delcamp, *J. Org. Chem.*, 2024, **89**, 9092–9097.
74 J. Liu, M. Liu, H. Zhang and W. Guo, *Angew. Chem., Int. Ed.*, 2021, **60**, 12992–12998.
75 M. Grzybowski, M. Taki, K. Kajiwara and S. Yamaguchi, *Chem.–Eur J.*, 2020, **26**, 7912–7917.
76 X. He, J.-B. Lin, W. H. Kan and T. Baumgartner, *Angew. Chem., Int. Ed.*, 2013, **52**, 8990–8994.
77 Z.-D. Li, F. Ren, Y. Wu, J.-J. Li, J. Luo and P. Wang, *Org. Lett.*, 2024, **26**, 7436–7441.
78 X. Zhang, J.-Q. Zhang, Z.-H. Sun, H.-M. Shan, J.-C. Su, X.-P. Ma, G.-F. Su, L.-P. Xu and D.-L. Mo, *Angew. Chem., Int. Ed.*, 2025, **64**, e202420390.
79 (*a*) CCDC 2478635: Experimental Crystal Structure Determination, 2025, DOI: **10.5517/ccdc.csd.cc2p66z3**.; (*b*) CCDC 2478637: Experimental Crystal Structure Determination, 2025, DOI: **10.5517/ccdc.csd.cc2p6716**.

© 2026 The Author(s). Published by the Royal Society of Chemistry